

## High-density MIM capacitors with HfO<sub>2</sub> dielectrics

Tsu-Hsiu Perng<sup>a,\*</sup>, Chao-Hsin Chien<sup>b</sup>, Ching-Wei Chen<sup>a</sup>, Peer Lehnen<sup>c</sup>, Chun-Yen Chang<sup>a</sup>

<sup>a</sup>Department of Electronics Engineering and Institute of Electronics, National Chiao-Tung University, Hsinchu 300, Taiwan, R.O.C.

<sup>b</sup>National Nano Device Laboratories, Hsinchu 300, Taiwan, R.O.C.

<sup>c</sup>AIXTRON AG, Aachen 52072, Germany

### Abstract

Metal–insulator–metal (MIM) capacitors with high-*k* HfO<sub>2</sub> dielectrics were fabricated and investigated. Experimental results show low leakage current densities of  $\sim 5 \times 10^{-9}$  A/cm<sup>2</sup> and high capacitance density of  $\sim 3.4$  fF/μm<sup>2</sup> at 100 kHz in the MIM capacitors. The temperature coefficient and frequency dispersion effect for these MIM capacitors were very small. Different metal electrodes like tantalum, aluminum and copper were also investigated and compared. Finally, the mechanism of electrical transport was extracted for the HfO<sub>2</sub> MIM capacitors to be Poole–Frenkel-type conduction mechanism.

© 2004 Elsevier B.V. All rights reserved.

*Keywords:* MIM capacitors; HfO<sub>2</sub>; Dielectrics

### 1. Introduction

In recent years, the dramatic increase in wired and wireless communications has demanded the need for high-quality passives for analog and mixed-signal applications. Metal–insulator–metal (MIM) capacitors using one of the standard back-end metal layers as bottom electrode have emerged as key passive components for microprocessors, high-frequency circuits and mixed-signal integrated circuits applications [1,2]. Compared with double polylinear capacitors, they offer the advantages of reduced series resistance and lower parasitic capacitance [3]. A high capacitance density is important for an MIM capacitor to increase the circuit density and reduce the cell area and cost. Therefore, adoption of high-*k* material like Al<sub>2</sub>O<sub>3</sub> or HfO<sub>2</sub> is a very efficient way to increase the capacitance density [4]. Silicon oxide and silicon nitride are dielectrics that are commonly used in conventional capacitors, but their capacitance densities are limited due to low dielectric constants. It is expected to be one solution to enhance the capacitance density by using higher dielectric constant materials.

Among various high-*k* dielectric candidates, HfO<sub>2</sub> has been investigated as a promising material in gate dielectric of MOSFETs due to its high dielectric constant, excellent thermal stability and high band gap. [5]. In addition, excellent MOS capacitors with HfO<sub>2</sub> have also been demonstrated [6]. Therefore, it seems that HfO<sub>2</sub> is a promising candidate for the above applications. In this work, MIM capacitors with HfO<sub>2</sub> dielectrics have been fabricated and investigated. Experimental results show low leakage current of  $\sim 5 \times 10^{-9}$  A/cm<sup>2</sup> and high capacitance density of  $\sim 3.4$  fF/μm<sup>2</sup> at 100 kHz in the MIM capacitors. The temperature coefficient and frequency dispersion effect for these MIM capacitors were very small. Different metal electrodes like tantalum, aluminum and copper were also investigated and compared. Finally, the mechanism of electrical transport was extracted for the HfO<sub>2</sub> MIM capacitors.

### 2. Experimental details

Standard 6-in. (150-mm) silicon wafers, with a resistivity of 15–25 Ω cm, were used in this study. An additional 500-nm thermal SiO<sub>2</sub> was grown on the Si substrate to increase the substrate isolation. The MIM capacitors with HfO<sub>2</sub> films

\* Corresponding author. Tel.: +886 3 571 2121; fax: +886 3 571 5506.

E-mail address: [thperng.ee88gnctu.edu.tw](mailto:thperng.ee88gnctu.edu.tw) (T.-H. Perng).

were subsequently formed on the 500-nm SiO<sub>2</sub>. Before high-*k* dielectrics deposition, a layer of Ta film was deposited by sputtering on SiO<sub>2</sub> as the bottom electrode. HfO<sub>2</sub> films (50 nm) were then prepared by sputtering in O<sub>2</sub> ambient. After that, a layer of Ta film was deposited as the top electrode. The pattern of the MIM capacitors was defined using a metal mask. The counterparts of the MIM capacitors with Al and Cu metals as the top electrodes were also fabricated for comparison. Finally, furnace annealing was conducted at 400 °C in N<sub>2</sub> ambient for 30 min.

The leakage current was measured using a Keithley Model 4200-SCS Semiconductor Characterization System, and the capacitance was measured using an Agilent 4284A precision LCR meter at frequencies varied from 1 kHz to 1 MHz. In order to investigate the thermal stability of the high-*k* dielectric film, thermal stresses were performed with measurement temperatures varied from 25 to 125 °C.

### 3. Results and discussion

Fig. 1 depicts the capacitance density as a function of applied voltage for HfO<sub>2</sub> at frequencies ranging from 1 kHz to 1 MHz. Both the top and bottom electrodes used here are Ta. The capacitor area in this measurement is  $2 \times 10^{-4}$  cm<sup>2</sup>. The capacitance densities decrease with frequency and are almost constant from -5 to 5 V. High capacitance value of 3.3 fF/μm<sup>2</sup> was measured at 100 kHz. The MIM capacitors using different top electrodes of Al, Ta and Cu are compared in Fig. 2. The capacitance densities depicted in Fig. 2 were measured at a frequency of 100 kHz. The capacitor with Al top electrode shows smaller capacitance density of 2.9 fF/μm<sup>2</sup>. This is reasonable because of the interfacial layer of Al<sub>2</sub>O<sub>3</sub> formed between HfO<sub>2</sub> and Al film during sample preparation. The overall capacitance was reduced by the lower dielectric constant of Al<sub>2</sub>O<sub>3</sub>. On the other hand, the capacitance

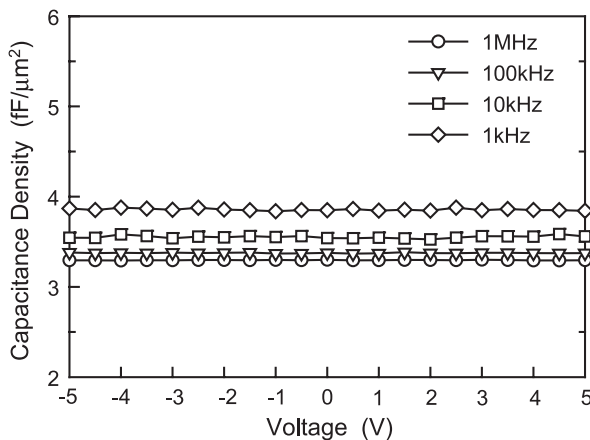


Fig. 1. Capacitance–voltage (*C–V*) characteristics of HfO<sub>2</sub> MIM capacitors with Ta electrodes at the frequencies from 1 kHz to 1 MHz.

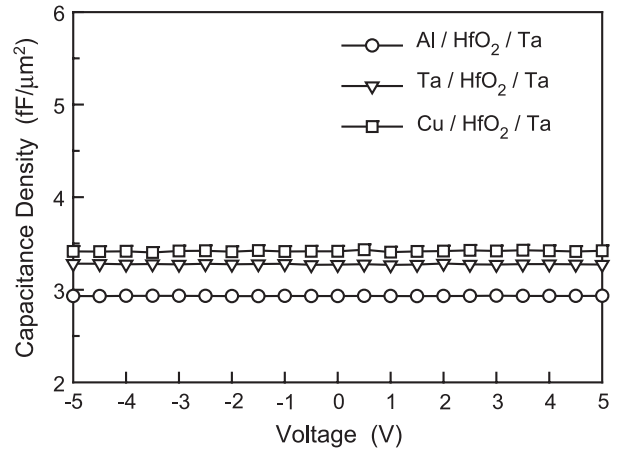


Fig. 2. Capacitance–voltage (*C–V*) characteristics of HfO<sub>2</sub> MIM capacitors with Al, Ta and Cu top electrodes at the frequency of 100 kHz.

density of the capacitor with Cu top electrode exhibits record high value of 3.4 fF/μm<sup>2</sup> in such thickness regime. The average voltage dependence of the MIM capacitor from 1 kHz to 1 MHz follows the voltage dependence of  $C_0 (\alpha \times V^2 + \beta \times V + 1)$ , where the voltage coefficients of capacitance (VCC) values of  $\alpha$  and  $\beta$  are listed in Table 1. The requirement of the quadratic coefficient of capacitance  $\alpha$  is smaller than 100 ppm/V<sup>2</sup>, and the requirement of the linear coefficient of capacitance  $\beta$  is below 1000 ppm/V according to the ITRS roadmap [7].

Fig. 3 shows the leakage current density–voltage (*J–V*) characteristics of HfO<sub>2</sub> MIM capacitors with different top electrodes of Al, Ta and Cu. The measured area is  $2 \times 10^{-4}$  cm<sup>2</sup> for all of the samples. The leakage current densities of the MIM capacitors exhibit nearly the same order of magnitude at low-field region. However, the current densities of the MIM capacitors with Ta and Cu top electrode show a little larger than that of the capacitor with Al top electrode after 2 V. Beyond 3 V, the current densities of the MIM capacitor with Cu top electrode increases obviously, while that of the capacitors with Al top electrode keeps the lowest current level until 5 V. The leakage current densities for the MIM capacitors with Al, Ta and Cu top electrodes are  $5.0 \times 10^{-9}$ ,  $7.8 \times 10^{-9}$  and  $9.0 \times 10^{-8}$  A/cm<sup>2</sup> at 5 V, respectively.

The loss tangent values as a function of frequency for the HfO<sub>2</sub> dielectric MIM capacitors with three different top electrodes are shown in Fig. 4. Similar trend in loss tangent values ( $1/Q$  factor) are observed for all of the samples. The lowest loss tangent value was measured at frequencies of 100 and 10 kHz. At frequencies of 1 MHz and 1 kHz, the loss tangent values increase to a value around 0.05.

Fig. 5 depicts the capacitance density of the MIM capacitor with Ta top electrode as a function of frequency after thermal stress from 25 to 125 °C. At lower temperature, the capacitance density decreases with frequency. However, this is not the case at elevated temperature. The

Table 1

Voltage linearity coefficients  $\alpha$  (ppm/V<sup>2</sup>) and  $\beta$  (ppm/V) as a function of frequency for the HfO<sub>2</sub> MIM capacitors with Ta, Al and Cu top electrode

Frequency	Tantalum (Ta)		Aluminum (Al)		Copper (Cu)	
	$\alpha$ (ppm/V <sup>2</sup> )	$\beta$ (ppm/V)	$\alpha$ (ppm/V <sup>2</sup> )	$\beta$ (ppm/V)	$\alpha$ (ppm/V <sup>2</sup> )	$\beta$ (ppm/V)
1 MHz	65.1	150.3	35.5	83.3	55.4	47.7
100 kHz	70.2	181.0	36.0	105.2	53.6	79.1
10 kHz	74.4	125.8	41.2	93.7	230.1	84.5
1 kHz	87.0	130.1	161.5	200.6	153.4	-33.7

capacitance density does not decrease monotonically with frequency but has a minimum at the frequency of 100 kHz. The same thermal stress measurement was conducted for the capacitor with Al and Cu top electrode, and the results are shown in Fig. 6. The tendency of the capacitance density for Al top electrode is similar to that for Ta top electrode. The capacitance density decreases initially and then increases with frequency for the case of Al top electrode. The poorer frequency dispersion for Al top electrode compared with that for Ta top electrode is probably the increased interface defect density around the interfacial layer formed at the less

stable Al/HfO<sub>2</sub> interface under the elevated temperature measurements. On the other hand, the capacitance density for Cu top electrode is obviously lowered at elevated temperatures. In addition, the capacitance density decreases with frequency at all thermal stress conditions. The major reason is considered to be the interface defect density increasing during the thermal stress process.

In order to elucidate the leakage mechanism, a plot of the leakage current density vs. the square root of the applied

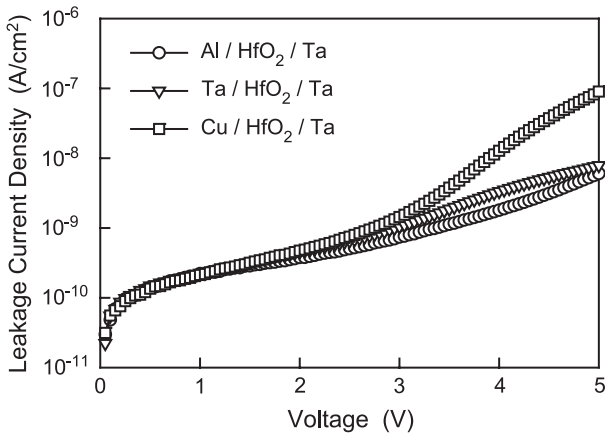


Fig. 3. Current density–voltage ( $J$ – $V$ ) characteristics of the HfO<sub>2</sub> MIM capacitors with the top electrodes of Al, Ta and Cu.

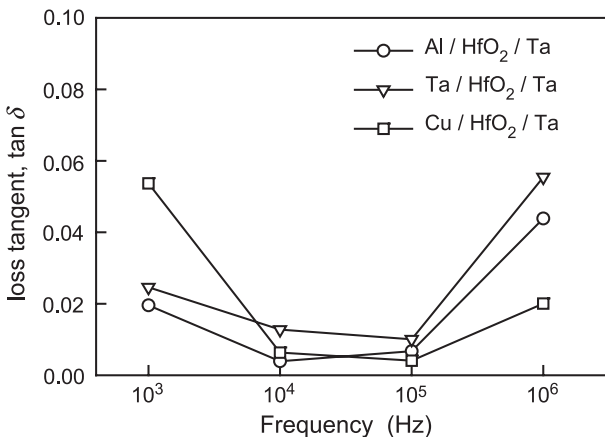


Fig. 4. Loss tangent as a function of frequency for the MIM capacitors with Al, Ta and Cu top electrodes.

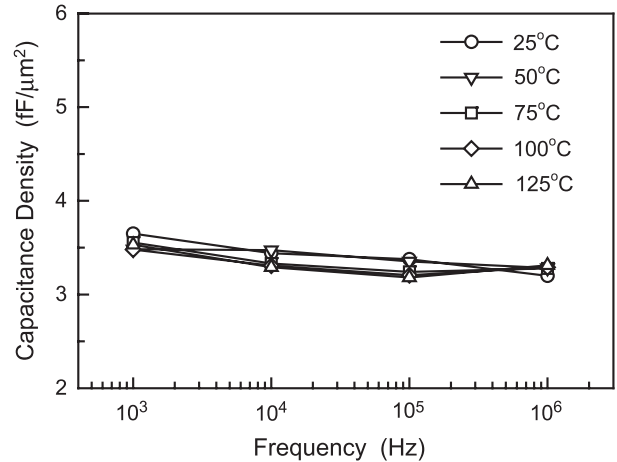


Fig. 5. Capacitance density of the MIM capacitor with Ta top electrode as a function of frequency after thermal stress from 25 to 125 °C.

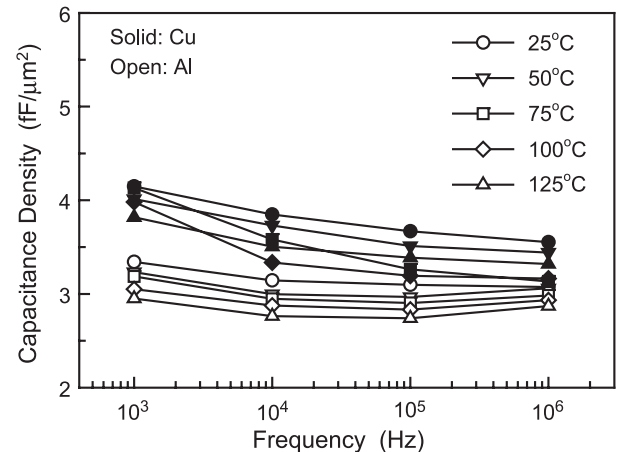


Fig. 6. Capacitance density of the MIM capacitor with Al and Cu electrode as a function of frequency after thermal stress from 25 to 125 °C.

electric field in the high electric field regime was sketched, as shown in Fig. 7. To make the plots concise and clear, only the high-field region is shown. Fig. 7a–c shows  $\ln(J/E)$  and  $E^{1/2}$  characteristics of the Ta/HfO<sub>2</sub>/Ta, Al/HfO<sub>2</sub>/Ta and Cu/HfO<sub>2</sub>/Ta MIM capacitors, respectively. We found that all leakage current densities of Ta, Al and Cu top electrode capacitors are increased with temperature, revealing a

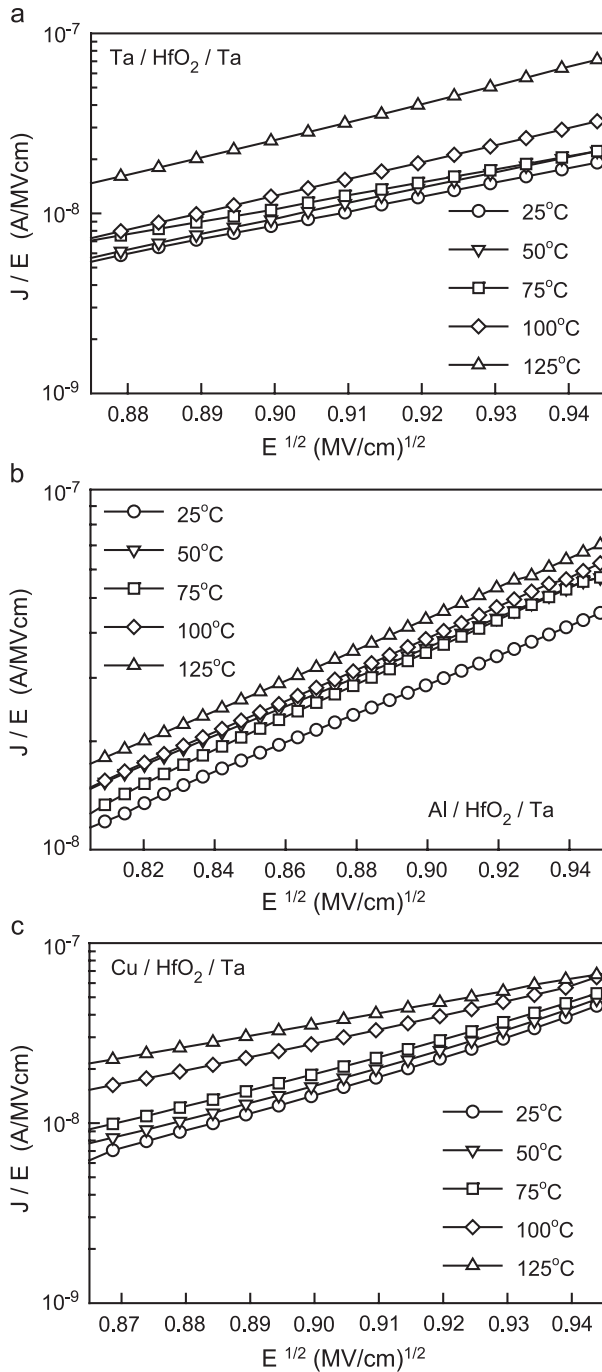


Fig. 7. Poole–Frenkel plot showing the current density vs. electric field characteristics at five measurement temperatures from 25 to 125 °C for HfO<sub>2</sub> MIM capacitor with (a) Ta top electrode, (b) Al top electrode and (c) Cu top electrode.

temperature dependence on the leakage behavior. In addition, all leakage current densities are linearly related to square root of the applied electric field. These linear variations of current densities, after careful calculation, correspond to Poole–Frenkel (PF)-type conduction mechanism [8],

$$J = J_0 \exp\left(\frac{\beta_{\text{PF}} E^{1/2} - \phi_{\text{PF}}}{k_{\text{B}} T}\right) \quad (1)$$

where  $J_0 = \sigma_0 E$  is the low-field current density,  $\sigma_0$  is the low-field conductivity,  $\beta_{\text{PF}} = (e^3 / \pi \epsilon_0 \epsilon)^{1/2}$ , and  $\phi_{\text{PF}}$  is the height of trap potential well. Rearrangement of Eq. (1) yields a linear relationship between  $\ln J$  and  $1/T$ , capable of calculating the height of trapping potential well  $\phi_{\text{PF}}$

$$\ln J = \ln(J_0) - \frac{1}{T} \left( \frac{\phi_{\text{PF}}}{k_{\text{B}}} - \frac{\beta_{\text{PF}} \sqrt{E}}{k_{\text{B}}} \right) \quad (2)$$

The values of  $e\phi_{\text{PF}}$  extracted from the slope of the equation are 0.95, 1.01 and 0.90 eV for Ta, Al and Cu top electrode, respectively. The calculated conduction mechanism of Poole–Frenkel type for all samples indicates that the current conduction is essentially via the trap state. However, some variation still exists in the extracted height of trap potential with respect to different top electrodes. This implies that the traps at and around the interface rather than the traps at deep level play the major role to the conduction mechanism.

#### 4. Conclusions

HfO<sub>2</sub> MIM capacitors with different metal top electrodes have been investigated. The MIM capacitor with Al top electrode exhibits the lowest capacitance density, while that with Cu top electrode exhibits the highest capacitance value of 3.4 fF/ $\mu\text{m}^2$ . Due to the Al<sub>2</sub>O<sub>3</sub> layer formed between Al and HfO<sub>2</sub>, the capacitance density and the leakage current density were reduced to 2.9 fF/ $\mu\text{m}^2$  and  $5.0 \times 10^{-9}$  A/cm<sup>2</sup> (at 5 V), respectively. On the other hand, although the MIM capacitor with Cu top electrode shows larger leakage current density at higher electric field, the successful fabrication of the Cu top electrode capacitor implies the possibility of integrating Cu with HfO<sub>2</sub> dielectrics. Thus, this indicates that it is very suitable for HfO<sub>2</sub> dielectric to use in silicon IC applications.

#### Acknowledgements

We are thankful for the technical support from National Nano Device Laboratories in National Applied Research Laboratories. This work was supported in part by the National Science Council of the Republic of China through contract No. NSC-92-2215-E-009-061.

## References

- [1] S. Decoutere, F. Vlegels, R. Kuhn, R. Loo, M. Caymax, S. Jenei, J. Croon, S.V. Huylenbroeck, M.D. Rold, E. Rosseel, P. Chevalier, P. Coppens, Proc. IEEE Bipolar/BiCMOS Circuits Technol. Meeting, 2000, p. 106.
- [2] M. Armacost, A. Augustin, P. Felsner, Y. Feng, G. Friese, J. Heidenreich, G. Hueckel, O. Prigge, K. Stein, Int. Electron Devices Meeting Tech. Dig., 2000, p. 157.
- [3] S. Jenei, S. Decoutere, S.V. Huylenbroeck, G. Vanhorebeek, B. Nauwelaers, Proc. IEEE Topical Meeting Si Monolithic IC in RF Systems, 2001, p. 64.
- [4] S.B. Chen, C.H. Lai, A. Chin, J.C. Hsieh, J. Liu, IEEE Electron. Device Lett. 23 (2002) 185.
- [5] G.D. Wilk, R.M. Wallace, J.M. Anthony, J. Appl. Phys. 89 (2001) 5243.
- [6] S.J. Lee, H.F. Luan, C.H. Lee, T.S. Jeon, W.P. Bai, Y. Senzaki, D. Roberts, D.L. Kwong, Proc. Symp. VLSI Tech., 2001, p. 133.
- [7] International Technology Roadmap for Semiconductors, Semiconductor Industry Assoc., 2001.
- [8] S.M. Sze, Physics of Semiconductor Devices, Wiley, New York, 1981, p. 402.